MMIC GaAs X-band Isolator with Enhanced Power Transmission Response

Andrea Ashley[1], Gregor Lasser[1], Zoya Popovic[1], Arjuna Madanayake[2] and Dimitra Psychogiou[1]
[1]Department of Electrical, Computer, and Energy Engineering, University of Colorado Boulder, Boulder, CO, USA
[2]Department of Electrical and Computer Engineering, Florida International University, Miami, FL, USA

***Abstract*—This paper discusses the RF design and characterization of an X-band MMIC isolator. It is based on a directional coupler and a non-reciprocal RF signal path that comprises a gain stage and two transmission line elements for phase control. In this manner, enhanced power transmission is obtained in the forward direction and isolation in the reverse one. The operating principles and RF design trade-offs (isolation, gain, matching) of the isolator are presented through circuit-based analysis. For proof-of-concept demonstration purposes, a prototype was designed at X-band and manufactured with a commercial MMIC GaAs process. Its RF measured performance is summarized as follows: center frequency: 9.4 GHz, maximum gain = 9.3 dB, maximum isolation = 27.7 dB, and 3 dB passband bandwidth with > 23 dB of isolation= 1.61 GHz.**

***Keywords*—Active isolator, gain stage, integrated circuit, MMIC isolator, non-reciprocity.**

I. INTRODUCTION

Non-reciprocal radio-frequency (RF) components, such as isolators and circulators form fundamental building blocks for microwave systems in which isolation between their front-end counterparts is critically important. They are used to protect high-power microwave sources, sensitive instrumentation systems and to separate the transmit and receive channels of full-duplex radios. While ferrite-based non-reciprocal RF components allow for high levels of isolation (IS ~35-70 dB) and moderate levels or insertion loss (IL ~1-3 dB) [1]-[3], their physical size is prohibitively-large for on-chip integration due to the need for external magnetic biasing.

Integrated isolators that exploit the inherent non-reciprocal properties of transistors are increasingly being explored as a compact and IC-compatible alternative [4]-[8]. Illustrative examples of these approaches include: i) two-port networks in which low noise amplifiers are combined with attenuators [4], ii) common base or common collector transistor-based configurations [5], and iii) the combination of non-reciprocal components with couplers [7]. While they exhibit small physical size and moderate-to-high-levels of isolation (20-37 dB), IL is present in their forward transmission. Furthermore, they are mostly limited to frequencies <6 GHz. Wideband active isolators have also been presented at X-band [8], however they present about 9 dB of IL in their forward direction.

Taking into consideration the aforementioned limitations, this paper focuses on the RF design and practical development of MMIC X-band isolators with enhanced power transmission in the forward direction and wide isolation in the reversed one. The content of this paper is organized as follows. Section II presents the operating and design principles of proposed active isolator through linear RF circuit analysis. The experimental validation of the isolator concept was performed at X-band using a commercial GaAs process and is reported in Section III. Lastly, the major contributions of this work are summarized in Section IV.

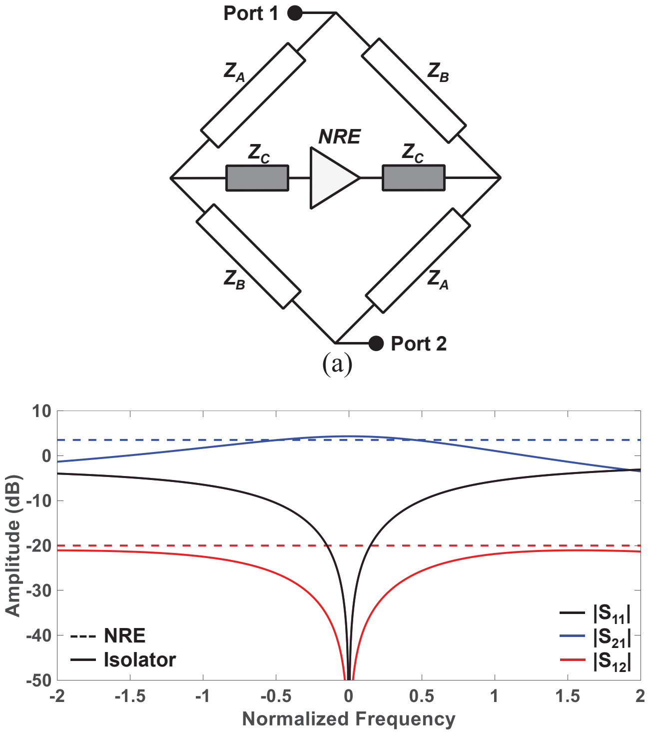

(a)

(b)

Fig. 1. RF isolator with enhanced power transmission response in the forward direction. (a) Block diagram, white and grey rectangles represent 90°-degree long transmission lines at $f_{cen,}$ white triangle: non-reciprocal element (*NRE*) with or without gain, (b) Ideal power transmission ($|S_{21}|$), isolation ($|S_{12}|$), and reflection ($|S_{11}|$) response of the isolator (solid lines) and its corresponding *NRE* (dashed lines). The element values for this example are as follows: $Z_A = 12\ \Omega$, $Z_B = 120\ \Omega$, $Z_C = 12\ \Omega$, *NRE* S-parameters: $S_{11} = 0$, $S_{12} = 0.1$, $S_{21} = 1.5$, and $S_{22} = 0$. $|S_{11}|$ and $|S_{22}|$ for the *NRE* are omitted.

II. DESIGN METHODOLOGY

The circuit details and operating principles of the integrated isolator concept are illustrated in Fig. 1. It is based on a directional coupler and a non-reciprocal RF signal path that is connected between the through- and reverse-coupled ports of the coupler. The coupler is shaped by two pairs of quarter-wavelength long transmission lines at f_{cen} with characteristic impedances Z_A and Z_B which control the matching and isolation. The non-reciprocal RF signal path comprises of a transistor-based non-reciprocal element (*NRE*) and additional phase-control elements (i.e., transmission lines with characteristic impedance Z_C and electrical length of 90-degrees at f_{cen}) whose parameters affect the matching, isolation and power transmission of the isolator. By appropriately selecting the gain of the *NRE*, the characteristics of the phase control element and the coupler, enhanced power transmission can be obtained in the forward direction and wide isolation in the reverse one. In particular, for given *NRE* characteristics (i.e., gain, isolation) the gain or isolation of the isolator can be designed to be larger. This is illustrated in Fig. 1(b) for an example case of a *NRE* with finite gain and isolation characteristics. As shown, by adding the coupler and the phase control elements, theoretically infinite isolation can be obtained at the center frequency of the isolator. Furthermore, its gain is larger than the one obtained in the *NRE*.

To better illustrate the operating principles of the active isolator concept, parametric studies altering the gain of the *NRE* and the impedances of the directional coupler (Z_A and Z_B) and Z_C were performed and are provided in Fig. 2. In these studies, the *NRE* is made from an ideal transistor that is matched at both ports and exhibits finite gain and isolation while the coupler is designed with a coupling factor equal to 0.01. In particular, Fig. 2(a) shows how Z_B alters the isolation, but keeps the gain and matching levels unaltered. Furthermore, the power transmission response can be designed with or without gain by altering the gain of the *NRE* as shown in Fig. 2(b). In a practical implementation concept, a pHEMT transistor can be used in the *NRE* in a common-source configuration and its gain can be altered by changing the DC biasing of its gate and drain. The matching levels of the isolator are mostly affected when Z_A and Z_C start to diverge from one another. This is demonstrated in Fig. 2(c), (d). In particular, Z_A primarily affects the match and isolation of the active isolator and Z_C affects the gain and matching levels.

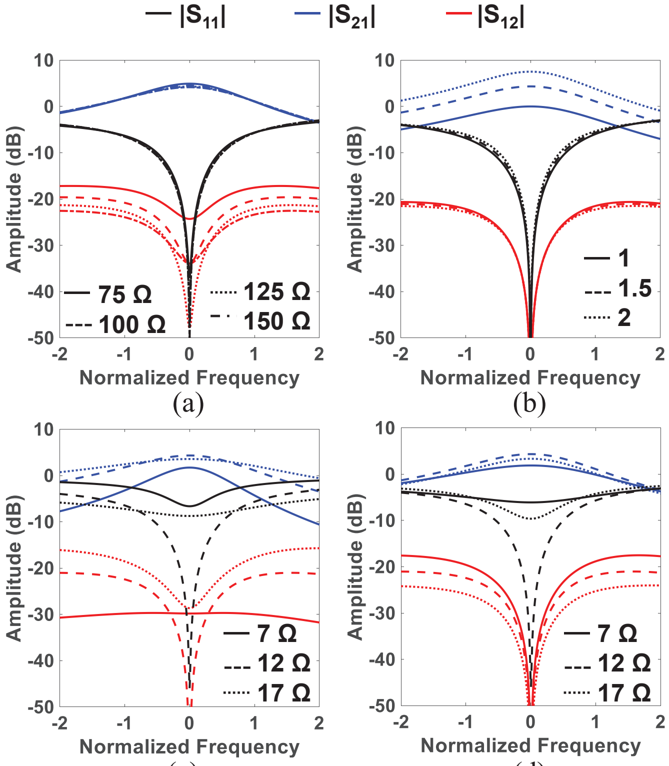

(a) (b)

(c) (d)

Fig. 2. RF power transmission (|S_{21}|), isolation (|S_{12}|), and reflection (|S_{11}|) response of the isolator as a function of: (a) Z_B, (b) Gain (S_{21}) of the *NRE*, (c) Z_A, and (d) Z_C. The rest of the circuit parameters are: Z_A = 12 Ω, Z_B = 120 Ω, Z_C = 12 Ω, *NRE* S-parameters: S_{11} = 0, S_{12} = 0.1, S_{21} = 1.5, and S_{22} = 0.

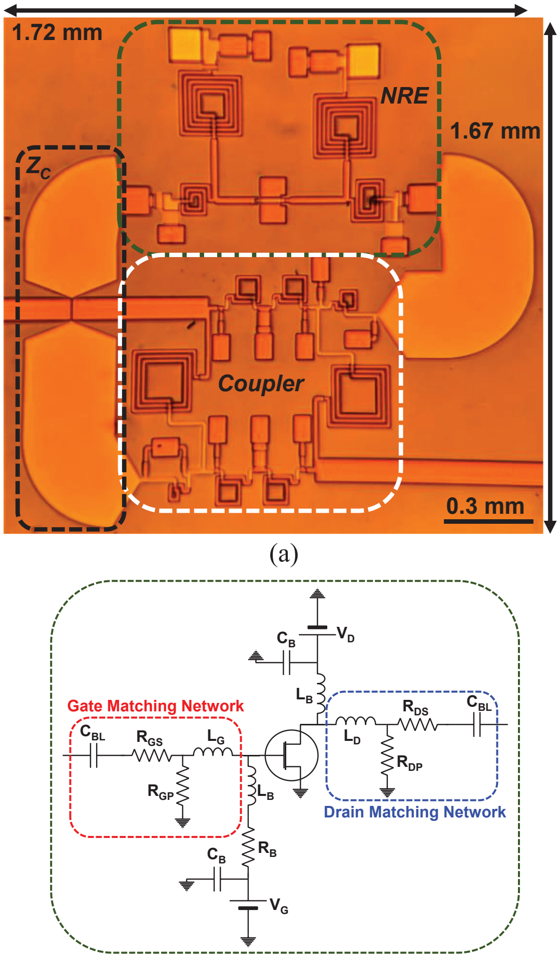

(a)

(b)

Fig. 3. (a) Photograph of the manufactured MMIC isolator prototype. The *NRE* is indicated in the green-enclosed area, the directional coupler (shaped by Z_A, Z_B) is indicated in the white-enclosed area, and the lines connecting the coupler and *NRE* are indicated in the black-enclosed area. (b) *NRE*. Its element values are as follows: C_{BL} = 3.2 pF, L_B = 13 nH, C_B = 2.1 pF, R_B= 10.1 Ω, R_{GS} = 21.6 Ω, R_{GP} = 45.1 Ω, L_G = 0.48 nH, L_D = 0.79 nH, R_{DS} = 10.1 Ω, R_{DP} = 45.5 Ω, V_G = 0.65V, and V_B = 2.5V.

III. EXPERIMENTAL VALIDATION

In order to evaluate the validity of the proposed isolator concept, a prototype was designed and manufactured at X-band using the WIN Semiconductor PIH1-10 GaAs process. It was designed for Z_A=23.5 Ω, Z_B=140 Ω and Z_C=27 Ω. A photograph of the prototype is shown in Fig. 3(a). Using as a reference the PIH1-10 GaAs stack-up, which consists of two metal layers, the

TABLE I. COMPARISON WITH STATE-OF-THE-ART ISOLATORS

Reference	**Topology**	***f*$_{cen}$ (GHz)**	**IS (dB)**	**$\|S_{21}\|$ (dB)**	**P$_{DC}$ (mW)**	**Size (λ x λ)**
[4]	Integrated, GaAs MMIC	1.4	31	-2.5	67.5	0.004 x 0.003
[5]	Integrated, SiGe	5.5	35	-2	2.5	0.012 x 0.008
[6]	Integrated, GaAs MMIC	3	30	-1.5	240	0.015 x 0.0075
[7]	Integrated, CMOS	24	36.8	-1.8	3.6	0.053 x 0.035
[8]	Integrated, MMIC	9.5	20	-9	30	N/A
This work	Integrated, GaAs MMIC	9.4	27.7	+9.3	68.75	0.054 x 0.052

RF input and output ports are designed on Metal 2 layer, while the additional transmission lines connecting the coupler to gain stage are on Metal 1 layer. The coupler was implemented through LE-based transmission lines and the transmission lines connecting the coupler to the amplifier stage were implemented in both microstrip and LE configurations for space conservation. The details of the *NRE* are shown in Fig. 3(b). It is made from a 2-finger pHEMT transistor biased at V_D=2.5V, and V_G=0.6 V and two matching networks that are respectively placed at the gain and drain.

The measured RF performance of the isolator was characterized in terms of S-parameters and is shown in Fig. 4. A comparison with the EM-simulated S-parameters is also provided and shows good agreement with the measured results, thus validating the proposed concept. The RF measured characteristics for this bias state (V_D=2.5V, and V_G=0.65V) are summarized as follows: center frequency (f_{cen}): 9.38 GHz, maximum gain ($|S_{21}|$): 9.3 dB, maximum IS: 27.7 dB, 3-dB BW with > 23 dB of isolation: 1.6 GHz, minimum 1-dB BW IS: 25.8 dB. Similar to the methods in Section II, in order to change the gain and isolation levels, the biasing of the *NRE* needs to be altered; this is shown in Fig. 5. By increasing the gate voltage, the gain is increased, however, the isolation in the reverse direction gets reduced. A comparison with state-of-art integrated isolators is provided in Table I. As shown, the proposed MMIC GaAs isolator is the only one designed with enhanced power transmission in its passband.

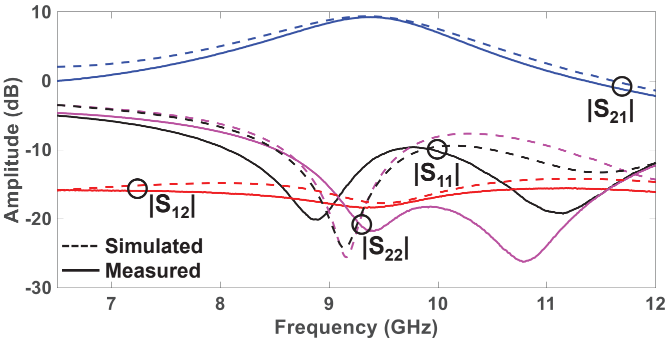

Fig. 4. RF-measured and EM-simulated S-parameters of the X-band isolator. The *NRE* was biased as follows: V_G=0.65 V and V_D=2.5 V.

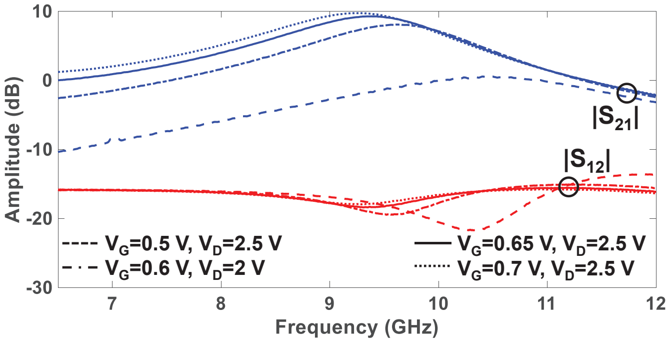

Fig. 5. Measured forward ($S_{21}|$) and reverse ($|S_{12}|$) power transmission for various bias states of the *NRE*.

IV. CONCLUSION

This paper reported on RF design and practical development of a fully-integrated X-band isolator using a commercially-available MMIC GaAs process. The operating principles of the proposed isolator were discussed using linear circuit analysis. They were validated experimentally with a proof-of-concept prototype at X-band that demonstrated high levels of isolation of about 27.7 dB and enhanced power transmission with a maximum gain of 9.3 dB.

ACKNOWLEDGMENT

This work has been supported in part by the National Defense Science and Engineering Graduate (NDSEG) Fellowship and the National Science Foundation under Grants ECCS-1731956 and ECCS-1941315. The authors acknowledge WIN Semiconductors Corp. for providing access to their PIH1-10 process and manufacturing test chips for the ECEN 5014 special topics class at the University of Colorado Boulder.

REFERENCES

[1] M. F. Farooqui, A. Nafe and A. Shamim, "Inkjet printed ferrite-filled rectangular waveguide X-band isolator," *2014 IEEE MTT-S International Microwave Symposium (IMS2014)*, Tampa, FL, 2014, pp. 1-4.

[2] J. Helszajn and M. Mckay, "Circular polarisation in a double-ridge waveguide," in *IEE Proceedings - Microwaves, Antennas and Propagation*, vol. 152, no. 1, pp. 25-30, 19 Feb. 2005.

[3] H. Dong, J. R. Smith and J. L. Young, "A wide-band, high isolation UHF lumped-element ferrite circulator," in *IEEE Microwave and Wireless Components Letters*, vol. 23, no. 6, pp. 294-296, June 2013.

[4] M. F. Cordoba-Erazo and T. M. Weller, "A 1.4 GHz MMIC active isolator for integrated wireless systems applications," *WAMICON 2014*, Tampa, FL, 2014, pp. 1-3.

[5] Jongsoo Lee, J. D. Cressler and A. J. Joseph, "A 5-6 GHz SiGe HBT monolithic active isolator for improving reverse isolation in wireless systems," in *IEEE Microwave and Wireless Components Letters*, vol. 15, no. 4, pp. 220-222, April 2005.

[6] D. G. Haigh, "Wideband active microwave isolators using GaAs MMIC technology," in *IEEE Proceedings - Microwaves, Antennas and Propagation*, vol. 143, no. 2, pp. 179-183, April 1996.

[7] Jen-Feng Chang, Jui-Chih Kao, Yu-Hsuan Lin and Huei Wang, "A 24-GHz fully integrated isolator with high isolation in standard RF 180-nm CMOS technology," *2014 IEEE MTT-S International Microwave Symposium (IMS2014)*, Tampa, FL, 2014, pp. 1-3.

[8] R. Pyndian and F. van den Bogaart, "Novel multioctave MMIC active isolator (1-20 GHz)," in *Electronics Letters*, vol. 25, no. 21, pp. 1420-1422, 12 Oct. 1989.